Peng *et al. Journal of Biological Engineering* (2025) 19:20
https://doi.org/10.1186/s13036-025-00489-w

Journal of Biological Engineering

RESEARCH Open Access

Carbon fluxes rewiring in engineered *E. coli* via reverse tricarboxylic acid cycle pathway under chemolithotrophic condition

Jian-Hau Peng[1,4,5,6], Shou-Chen Lo[2], Yu-Ning Yu[2,6], Ya-Tang Yang[3], Yu-Chieh Chen[2], An-I Tsai[2], Dong-Yan Wu[2], Chu-Han Huang[2], Tien-Tsai Su[2], Chieh-Chen Huang[1,2,4,5*] and En-Pei Isabel Chiang[1,4,5,6*]

Abstract

Background A transgenic strain of *Escherichia coli* has been engineered to directly assimilate gaseous CO_2 into its biomass through hydrogen-powered anaerobic respiration. This was achieved by expressing key components of the reverse tricarboxylic acid (rTCA) cycle, including genes encoding α-ketoglutarate: ferredoxin oxidoreductase (KOR) and ATP-dependent citrate lyase (ACL) from *Chlorobium tepidum*. These enzymes were selected for their essential roles in enabling CO_2 fixation and integration into central metabolism.

Results This study found that KOR alone can support cellular maintenance under chemolithotrophic conditions, while additional expression of ACL enhances CO_2 assimilation. Using isotopic $^{13}CO_2$ tracing, it was demonstrated that KOR alone facilitates CO_2 assimilation into TCA metabolites. However, co-expression of ACL with KOR redirected carbon fluxes from TCA cycle toward essential metabolic pathways, particularly those involved in protein and nucleotide biosynthesis. Compared to KOR alone, ACL co-expression significantly increased isotopic enrichments in amino acids (e.g., methionine, threonine, glycine) and nucleotides (e.g., deoxythymidine, deoxycytidine). These results suggest that ACL supports the synthesis of nitrogen-containing metabolites when inorganic nitrogen is sufficient, while KOR alone sustains core metabolic functions under chemolithotrophic conditions.

Conclusions This study demonstrates a novel strategy to engineer *E. coli* for CO_2 fixation using only one or two heterologous enzymes under chemolithotrophic conditions. These findings reveal the minimal genetic and nutritional requirements for CO_2 assimilation and provide insights into metabolic flux partitioning in engineered strains. This research paves the way for sustainable applications in carbon fixation and biotechnological innovation.

Keywords *Escherichia coli*, Reverse tricarboxylic acid cycle, Carbon flux rewiring, CO_2 incorporation, Protein and nucleotide biosynthesis

*Correspondence:
Chieh-Chen Huang
cchuang@dragon.nchu.edu.tw
En-Pei Isabel Chiang
chiangisabel@nchu.edu.tw
Full list of author information is available at the end of the article

© The Author(s) 2025. **Open Access** This article is licensed under a Creative Commons Attribution-NonCommercial-NoDerivatives 4.0 International License, which permits any non-commercial use, sharing, distribution and reproduction in any medium or format, as long as you give appropriate credit to the original author(s) and the source, provide a link to the Creative Commons licence, and indicate if you modified the licensed material. You do not have permission under this licence to share adapted material derived from this article or parts of it. The images or other third party material in this article are included in the article's Creative Commons licence, unless indicated otherwise in a credit line to the material. If material is not included in the article's Creative Commons licence and your intended use is not permitted by statutory regulation or exceeds the permitted use, you will need to obtain permission directly from the copyright holder. To view a copy of this licence, visit http://creativecommons.org/licenses/by-nc-nd/4.0/.

Background

The commitment to achieving net zero carbon emissions by 2050 and implementing carbon border adjustment mechanisms have elevated CO_2 fixation to a prominent topic, particularly within the field of life sciences [1]. The development of genetic pathways for CO_2 fixation and the reconfiguration of carbon fluxes have become a critical issue. Modern synthetic biotechnology and metabolomics advancements have facilitated more effective strategies to redesign and trace the CO_2 fluxes into specific target compounds.

Autotrophic bacteria play a vital role in ecosystems by continuously supplying organic carbon to heterotrophs through CO_2 fixation [2]. However, their limited carbon fixation efficiency, slow growth rates, and dependence on extreme environmental conditions restrict their adaptability as cell factories [3]. Chemolithotrophs are a diverse group of microbes capable of deriving all the energy needed for growth by oxidizing inorganic compounds such as hydrogen (H_2), hydrogen sulfide (H_2S), and reduced metals [4–7]. By contrast, *Escherichia coli* presents several advantages for metabolic engineering applications, including rapid growth, substrate versatility, and ease of genetic manipulation [8]. The fixation of CO_2 into living matter supports all life on earth. In early earth, the last universal common ancestor (LUCA) and autotrophic microbes, including archaea, could fix CO_2 under extreme conditions with minimal inorganic nutrients [9]. At least six types of autotrophic carbon-fixation pathways have been identified across the tree of life, including (1) reductive acetyl-CoA pathway (Wood–Ljungdahl pathway) in some strict anaerobic Proteobacteria, Planctomycetes, spirochaetes and Euryarchaeota [10–14]; (2) 3-hydroxypropionate bicycle in some green non-sulphur bacteria of the family Chloroflexaceae [15–18]; (3) 3-hydroxypropionic acid/4-hydroxybutyrate cycle in aerobic Crenarchaeota [19]; (4) dicarboxylate-4-hydroxybutyrate cycle in anaerobic Thermoproteales and Desulfurococcales [20–22], (5) reductive pentose phosphate cycle (Calvin–Benson–Bassham (CBB) cycle) in plants, algae, cyanobacteria, some aerobic or facultative anaerobic Proteobacteria, *Sulfobacillus* and *Oscillochloris* [23–26]; and (6) reverse tricarboxylic acid (rTCA) cycle (Arnon–Buchanan cycle) in green sulfur bacterium [20, 27–30].

Among these, the CBB cycle is the most significant autotrophic carbon fixation pathway in plants and algae [2, 31–33]. Compared to the CBB cycle, rTCA cycle appears more efficient for CO_2 fixation in microorganisms [27, 30, 34], and the rTCA cycle is considered a plausible candidate for the earliest autotrophic metabolism at the origin of life [35]. Its origins are proposed to predate the advent of enzymes, ribonucleic acid (RNA), or cells, with its imprint remaining inherently embedded in the core metabolic structure [36]. Modern theories suggest that the origin of life involved a dynamic process through the intermediacy of five essential universal metabolites—acetate, pyruvate, oxaloacetate, succinate, and α-ketoglutarate—comprising carbon, hydrogen, and oxygen [37, 38]. Muchowska et al. described a purely chemical reaction network promoted by ferrous iron involving aqueous pyruvate and glyoxylate, two products of abiotic CO_2 reduction. This network could synthesize nine of the eleven biological tricarboxylic acid (TCA) cycle intermediates, including all five universal metabolic precursors [38]. The observed network overlaps substantially with the TCA and glyoxylate cycles [38] and may represent a prebiotic precursor to these core metabolic pathways. Among these universal pathways, we proposed that the carboxylation of succinyl-CoA to α-ketoglutarate, catalyzed by α-ketoglutarate: ferredoxin oxidoreductase (KOR, encoded by genes of two sub-units: *korA* and *korB*), is the most relevant to early autotrophic life for the following reasons: (a) it operates in phylogenetically diverse, extreme-environmental autotrophic bacteria [2]; (b) it is a crucial step in carboxylation within the rTCA cycle, necessary for driving this cycle; and (c) α-ketoglutarate plays a central role in this metabolic network [39]. KOR was selected as the primary entry for carbon incorporation due to its position at the intersection of anabolic and catabolic pathways. Additionally, ATP-dependent citrate lyase (ACL, encoded by genes of two sub-units: *aclB* and *aclA*) was included in our carbon-fixing model to catalyze the cleavage of citrate into acetyl-CoA and oxaloacetate, potentially providing key carbon sources for downstream metabolites.

The rTCA machinery has been successfully constructed in *E. coli* through the expression of ten genes encoding four irreversible enzymes of the TCA cycle in wildtype *E. coli* JM109 (Fig. 1a), derived from the phototrophic green sulfur bacterium *Chlorobium tepidum* [40]. The recombinant *E. coli* harboring these ten genes demonstrated CO_2 assimilation capabilities, evidenced by a reduction in CO_2 release. However, the specific roles of KOR and ACL in redirecting carbon fluxes have yet to be fully elucidated.

This study aimed to identify the minimal gene set and nutritional conditions required for CO_2 assimilation in heterotrophic *E. coli* using the rTCA machinery. The carbon flow and the partitioning among critical metabolic fluxes under such limited conditions was also investigated, providing insights into the essential carboxylation pathways in a heterotrophic host. The study also presents a novel strategy for engineering *E. coli* to not only assimilates external gaseous CO_2 but also to redirects and

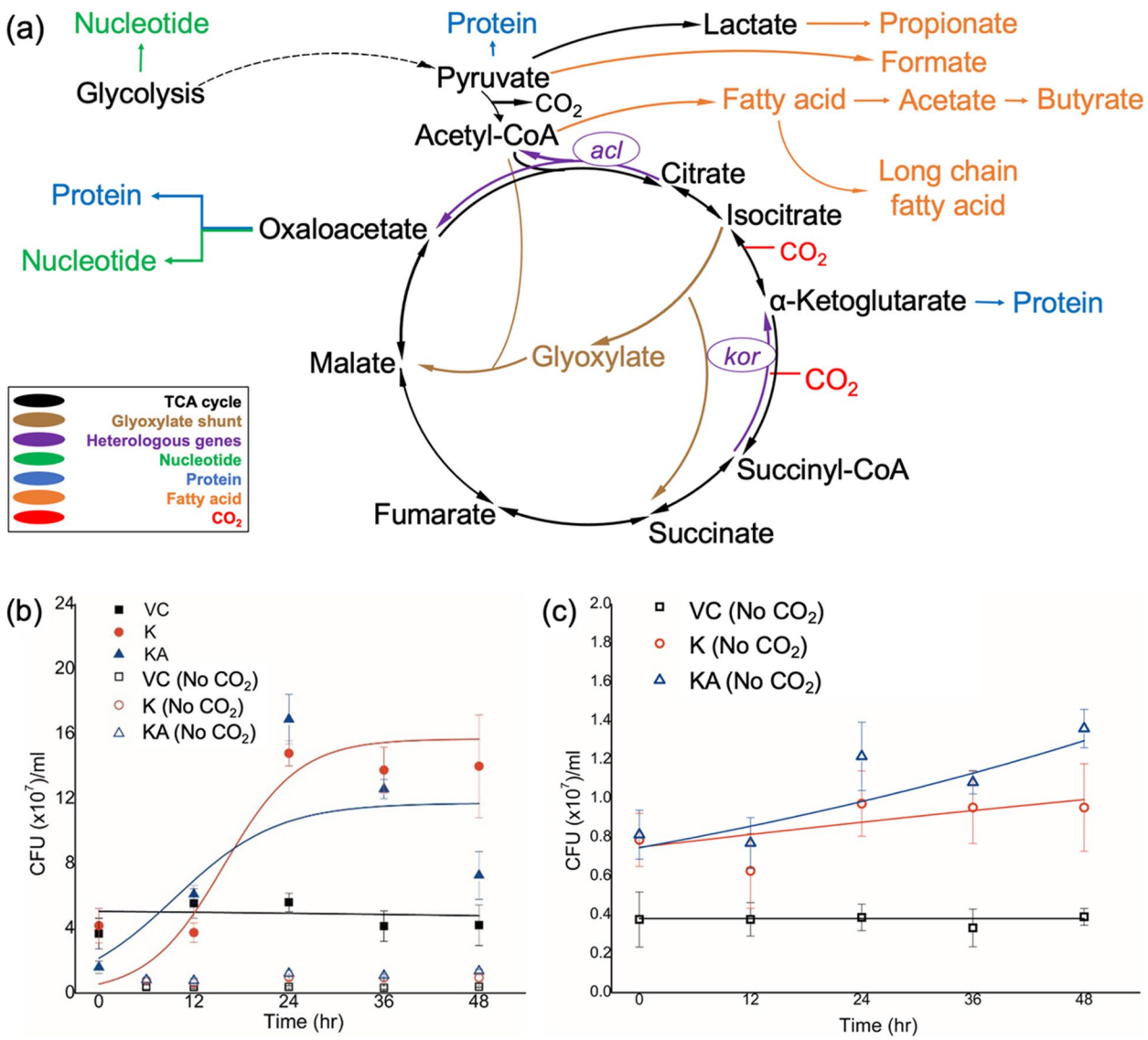

Fig. 1 **a** The pathways of central carbon metabolism, TCA cycle, fatty acid synthesis, and genetic engineering strategy.**b** The growth curves of transgenic *E. coli* K12 with different gene sets expression under organic-free medium supplied with 0.5% DMSO, 0.00005% thiamine, H_2 gas, without any amino acid in the presence or absence of CO_2. **c** Enlarged view of growth curves under organic-free medium in the absence of CO_2. The DNA cassettes used to construct expression plasmids pGETS-K and pGETS-KA which encode genes *korA* and *korB*, *aclB* and *aclA* form *C. tepidum*. Data are expressed as means standard ± deviation, $n = 3$ independent biological samples

concentrates carbon flow towards the production of valuable target metabolites.

Materials and methods

Chemicals and materials

Luria-Bertani broth was obtained from Cyrusbioscience, Inc. (New Taipei City, Taiwan). M9 minimal medium was sourced from Becton, Dickinson and Company (East Rutherford, USA). Casein hydrolysate, $FeCl_2$, aspartic acid, sodium nitrate, ^{13}C-CO_2, chloroform, methoxymation hydrochloride, N-tert-Butyldimethylsily-N-methyltrifluoroacetamide (MTBSTFA), pentafluorobenzyl bromide (PFBBr), and methanolic sodium hydroxide were procured from Sigma-Aldrich (Merck Group, St. Louis, USA). Dimethyl sulfoxide (DMSO), thiamine and $NiCl_2$ were procured from Acros Organics (Thermo Fisher Scientific Inc., Waltham, USA). $MgSO_4$ was obtained from Wako Pure Chemical Industries, Ltd. (Osaka, Japan). $CaCl_2$ and methanol were purchased from Aencore Chem. Pty. Ltd. (City of Whitehorse, Australia). Chloramphenicol was acquired from Bio Basic Inc. (Markham, Canada). Glucose was purchased from Showa Chemical Industry Co., Ltd. (Tokyo, Japan). Tris

buffer was obtained from MDBio, Inc. (New Taipei City, Taiwan). [$^{13}C_3$]-pyruvate, [$^{13}C_3$]-lactate, [$^{13}C_4$]-succinate, [$^{13}C_4$]-fumarate, [$^{13}C_4$]-malate, [1,5,6-carboxyl-$^{13}C_3$]-citrate and ^{13}C-formate were sourced from Cambridge Isotope Laboratories, Inc. (Tewksbury, USA). BCl_3-methanol solution was purchased from Supelco (Merck Group, Bellefonte, USA). Sodium chloride was obtained from Panreac Química SLU (Barcelona, Spain). HCl was purchased from Biosynth Ltd. (Staad, Switzerland). Formic acid was acquired from J. T. Baker (Mallinckrodt Baker, Inc., Phillipsburg, USA). N, O-bis-[trimethylsilyl] trifluoroacetamide 1% trimethylchlorosilane was sourced from Pierce Biotech (Thermo Fisher Scientific Inc., Waltham, USA). Acetonitrile, n-hexane and acetone were purchased from ECHO Chemicals Co. Ltd. (Miaoli County, Taiwan). DB-225MS, DB-225 J&W GC, CP-Sil and HP-5MS columns were obtained from Agilent Technologies Ltd. (Santa Clara, USA).

Construction of the transgenic strains

The construction of the transgenic strains used in this study followed the methodology described in a previous work employing the Ordered Gene Assembly in the *Bacillus subtilis* (OGAB) method [41, 42] with modifications detailed in [40]. The designed 3'-tail deoxyribonucleic acid (DNA) cassettes, which contain three complementary nucleotides for the OGAB method, were amplified using the primer pairs KOR-DraIII-f/KOR-PflMI-tail-r and ACL-PfMI-f/ACL-PflMI-tail-r. These primers encode α-ketoglutarate: ferredoxin oxidoreductase and ATP-dependent citrate lyase from plasmid pGETS-KA. Plasmid pGETS-K was constructed with the DNA cassette amplified using the KOR-DraIII-f/KOR-PflMI-tail-r primer pair. Plasmid pGETS-KA was constructed with DNA cassettes amplified using the KOR-DraIII-f/KOR-DraIII-r and ACL-PfMI-f/ACL-PflMI-tail-r primer pairs. The DNA cassettes of the constructed plasmids were verified by sequencing (Genomics, New Taipei City, Taiwan). The constructed strains and primers are listed in Table 1a.

Microbial incubation and counting

Microbial samples were incubated and collected according to the procedure described previously [40]. The *E. coli* strains were cultured at 37 °C in Luria-Bertani broth for 12 h, washed with M9 minimal medium and collected. The bacteria were concentrated to an optical density (O.D.) of 5 at 600 nm and inoculated (1%, v/v) into 150 mL of organic-free medium (M9 minimal medium with 0.01 M $NaNO_3$, 2 mM $MgSO_4$, 0.1 mM $CaCl_2$, 0.01 mM $NiCl_2$, 0.01 mM $FeCl_2$ and 20 μg/mL chloramphenicol) in a sealable glass bottle. The medium was prepared in an anaerobic chamber (Coy Laboratory Products, Inc., USA) and sealed with robber and aluminum caps (Shang-Jhan Class Instrument Co., Hsinchu City, Taiwan) for anaerobic experiments.

The headspace for each bottle (100 mL) was filled with hydrogen and CO_2 (90% H_2, 10% CO_2). To elucidate the role of *korAB* and *aclBA* genes, two transgenic strains, namely strain KA (*korAB*+*aclBA*) and strain K (*korAB*), were cultured in the organic-free medium. The CO_2 gas was refilled every 12 h during incubation.

In the isotopic labeling experiment, gaseous CO_2 was replaced with $^{13}CO_2$. Bacterial growth was assessed by measuring optical density (GeneQuant 1300, GE Healthcare, Little Chalfont, Buckinghamshire, UK) or counting colony-forming units (cfu).

Enzyme assays

The *E. coli* strains were incubated in M9 medium supplied with 2 g/L glucose, 2 mM $MgSO_4$, 0.1 mM $CaCl_2$, 50 μg/mL thiamine, 20 μg/mL chloramphenicol, and 1 g/L casein hydrolysate under anaerobic conditions. The headspace of the bottle was purged with H_2 and CO_2 and sealed with rubber to maintain the anaerobic conditions. For anaerobic respiration conditions, glucose and casein hydrolysate were replaced with 10 mM sodium nitrate, 0.01 mM $NiCl_2$, and 0.01 mM $FeCl_2$. Approximately 4×10^9 bacteria cells were collected from 150 mL of glucose medium or 750 mL anaerobic respiration medium and sonicated in Tris buffer (100 mM Tris-HCl at pH 8.4, 3 mM dithioerythritol). The crude proteins were collected from the supernatant by centrifugation at 10,000 ×g. Methyl viologen assays were performed in an anaerobic chamber filled with 9% H_2, 15% CO_2, and 76% N_2 gas at 35 °C, and optical densities were measured. Enzyme activities were assessed using a Jasco V-630 UV-Vis spectrophotometer (JASCO, Tokyo, Japan) equipped with a temperature controller (Water Bath D-606, Deng Yng, New Taipei City, Taiwan).

α-Ketoglutarate oxidoreductase activity assays

The activity of α-ketoglutarate oxidoreductase was assessed using a modified method described previously [43]. The enzyme activity was determined by monitoring succinyl-CoA reduction (reduced methyl viologen: succinyl-CoA oxidoreductase). The assay was conducted in a 1 mL reaction mixture containing 100 mM Tris-HCl at pH 8.4, 2 mM $MgCl_2$, 4 mM methyl viologen, and 1 mM succinyl-CoA. Dithionite was added from a 1 M stock solution until the methyl viologen-containing assay solutions exhibited a faint blue color. Optical density changes were measured at 578 nm (methyl viologen, $\varepsilon_{578}=9.8\times10^3\ M^{-1}\ cm^{-1}$) after the addition of the succinyl-CoA solutions.

Table 1 (**a**) The primers employed for constructing the pGETS118-reverse tricarboxylic acid plasmid. (**b**) Differential gene expression in the constructed *E. coli* strains K or KA/VC under incubation with CO_2 as the sole carbon source

(a)

Strains, plasmids, primers[a]	Genotype, phenotype, or sequence of primer (5′ to 3′)[b]	Origin
E. coli K12 BW25113	F-, Δ(*araD-araB*)567, Δ*lacZ4787*(::*rrnB*-3), λ⁻, *rph*-1, Δ(*rhaD-rhaB*)568, *hsdR514*	Parent strain for Keio Collection
Strain VC	*E. coli* K12 BW25113 contains plasmid VC	This study
Strain KA	*E. coli* K12 BW25113 contains plasmid KA	This study
Strain K	*E. coli* K12 BW25113 contains plasmid K	This study
Plasmid VC	pGETS118SfiI-pR, Tc^r, CAT^r	[41]
Plasmid KA	Plasmid VC with *korAB-aclBA* inserted after pR promoter	This study
Plasmid K	Plasmid VC with *korAB* inserted after pR promoter	This study
KOR-DraIII-f	ATGCAC**GTT**GTGGAAAAAAGGAAGAGGGGATACCCATGAGTGAC	[40]
KOR-PflMI-tail-r	ATGCCAAA**AGA**TTGGTCAGTTGATCGTCCAGGTGCTGTTGC	This study
KOR-DraIII-r	ATGCAC**AGT**GTGTCAGTTGATCGTCCAGGTGCTGTTGC	[40]
ACL-PflMI-f	ATGCCAAA**ACT**TTGGATAATATAAACATATAGAGCATGGCTAAAATTCTTGAAGG	[40]
ACL-PflMI-tail-r	ATGCCAAA**AGA**TTGGTTACTTCTTGTCGGGAACCG	This study
ACL-PflMI-r	ATGCCAAA**CAT**TTGGTTACTTCTTGTCGGGAACCG	[40]

(b)

Gene name	Description	Log2 Ratio[c,d]	
		Strain K/VC	Strain KA/VC
Heterologous expression (*C. tepidum* genes cloned into *E. coli* K12)			
aclA (CT1088)	ATP-citrate lyase α subunit	0.00	19.40
aclB (CT1089)	ATP-citrate lyase β subunit	0.00	20.67
korB (CT0162)	α-oxoglutarate ferredoxin oxidoreductase subunit β subunit	22.66	22.82
korA (CT0163)	α-oxoglutarate ferredoxin oxidoreductase subunit α subunit	12.79	12.28

[a] DraIII and PflMI indicated which restriction enzyme was used for OGAB method

[b] Underlined bases represent restriction sites for DNA cloning. Bolded bases represent the designed three complementary nucleotides for OGAB method to DNA fragments

[c] Differential gene expression was analyzed with Student's t-test and the false discovery rate, and both p-values < 0.05 are shown

[d] The transcription levels of heterologously expressed genes in the control strain were set as 0.001

Isocitrate dehydrogenase activity assay

Isocitrate dehydrogenase activity was measured by the reductive carboxylation of α-ketoglutarate [44]. The assay was performed in a reaction mixture containing 100 mM potassium phosphate buffer (pH 6.5), 0.6 mM α-ketoglutarate, 0.5 mM Nicotinamide adenine dinucleotide phosphate (NADPH), 1 mM $MnCl_2$, and 20 mM $NaHCO_3$. Optical density changes were measured at 340 nm (NADPH, $\varepsilon_{340} = 6.22 \times 10^3\ M^{-1}\ cm^{-1}$) following the addition of NADPH.

Isocitrate lyase activity assay

Isocitrate lyase activity was determined by the formation of glyoxylate-phenylhydrazone ($\varepsilon_{324} = 16.8 \times 10^3\ M^{-1}\ cm^{-1}$) [45], coupled with intrinsic aconitase. The assay was conducted in a reaction mixture containing 100 mM Tris-HCl (pH 7.1), 7.5 mM $MgCl_2$, 5 mM phenylhydrazine-HCl, 3 mM cysteine-HCl, and 2 mM sodium citrate. Optical density changes were measured at 324 nm following the addition of sodium citrate.

Succinyl-CoA synthetase activity assay

Succinyl-CoA synthetase activity was measured by monitoring the formation of thioester bonds of succinyl-CoA ($\varepsilon_{235} = 4 \times 10^3\ M^{-1}\ cm^{-1}$) [46]. The assay was conducted in a reaction mixture containing 100 mM Tris-HCl (pH 7.1), 2 mM 2-mercaptoethanol, 10 mM $MgCl_2$, 0.375 mM adenosine triphosphate (ATP), 0.1 mM coenzyme A, and 50 mM sodium succinate dibasic. Optical density changes were measured at 235 nm following the addition of sodium succinate dibasic.

Determination of TCA cycle metabolite enrichments and concentration

The TCA cycle metabolites from microbial samples were extracted using methanol and chloroform with an internal standard mixture ([$^{13}C_3$]-pyruvate, [$^{13}C_3$]-lactate, [$^{13}C_4$]-succinate, [$^{13}C_4$]-fumarate, [$^{13}C_4$]-malate and [1,5,6-carboxyl-$^{13}C_3$]-citrate). The polar metabolites (upper phase) were freeze-dried and derivatized using methoxymation hydrochloride and MTBSTFA. The metabolite derivatives were separated

on a DB-225MS column (30 m × 0.25 mm) and analyzed in electron ionization mode by gas chromatography-mass spectrometry (GC-MS) using a model 6890 gas chromatograph and model 5973 mass spectrometer (Agilent Technologies Ltd., Santa Clara, USA). The results were quantitated by referencing the standard curve for each TCA cycle metabolite. The coefficient of determination (r^2) for the standard curve was consistently greater than 0.99 [47, 48].

Extraction and quantitation of short-chain fatty acids in microbes

The short-chain fatty acids (SCFAs) from microbial samples were extracted and derivatized using 100 mM PFBBr in acetone in the presence of a working buffer (0.5 M phosphate buffer (pH 8.0) and a standard solution of sodium ^{13}C-formate (1 mM sodium ^{13}C-formate) in HPLC-grade water. n-hexane was used to separate polar and nonpolar metabolites from the extracted samples. The SCFAs in the organic phase were converted to alkylated derivatives and separated using a DB-225 J&W GC column (30 m × 0.25 mm). Mass spectrometry (MS) was performed in electron impact ionization mode, monitoring m/z at 226, 227, 240, 254, and 268 for formate, internal standard, acetate, propionate, and butyrate, respectively. The SCFAs were quantified by GC-MS using electron ionization mode. The results were quantitated by referencing a standard curve with known concentrations of SCFA standards plotted against the ^{12}C/^{13}C-formate ratio on the y-axis. The coefficient of determination for the standard curve was consistently greater than 0.99 [49].

Determination of fatty acid profile in microbes

Fatty acids from the microbial samples were extracted using a chloroform/methanol mixture (1:2) on ice, along with an internal standard ($C_{19:0}$ in ethanol) [50]. The nonpolar metabolites were freeze-dried and esterified using methanolic sodium hydroxide at 100 °C. They were then extracted using BCl_3-methanol solution (12%), saturated aqueous sodium chloride, and n-hexane [51, 52]. The fatty acids were converted to methyl ester derivatives and separated on a CP-Sil column (50 m × 0.25 mm). Their composition was determined by GC-MS in electron ionization mode [52–55].

Determination of amino acid profile and enrichments

Microbial pellets were collected from the broth by centrifugation (10,000 ×g) at 4 °C after incubation. The protein pellets were hydrolyzed using 6 N HCl under vacuum. Amino acids were then converted to heptafluorobutyryl n-propyl ester derivatives and separated on an HP-5MS column (30 m × 0.25 mm). Isotopic enrichment of amino acids was determined using GC-MS in electron capture negative ionization mode, as described previously [56, 57].

Determination of deoxyribonucleic acid metabolites enrichments

The microbial pellets were collected from the broth by centrifugation (10,000 ×g) at 4 °C after incubation. DNA samples were dried and hydrolyzed in formic acid under vacuum, then derivatized by N, O-bis-[trimethylsilyl] trifluoroacetamide 1% trimethylchlorosilane and acetonitrile. The resulting trimethylsilane-base derivatives were separated on an HP-5MS column. Isotopic enrichments in deoxyadenylate (dAMP, dA), deoxyguanylate (dGMP, dG), deoxythymidine (dTMP, dT), and deoxycytidine (dCMP, dC) were determined in positive ionization mode by GC-MS, as described previously [56, 58].

Statistical analysis

Comparisons of the means between the control and the experimental strains were conducted using the Student's t-test and Mann-Whitney U test. To examine statistical difference among the transgenic strains, a one-way ANOVA model followed by Tukey's post hoc test was employed. All statistical analyses were performed using SYSTAT 11.0 for Windows™ (Systat software Inc., Richmond, CA, USA). The results were deemed statistically significant if p values were <0.05, and borderline significance was considered for p values <0.1.

Results and discussion

The present study provides new insights into the role of KOR in supporting transgenic *E. coli* under chemolithotrophic mode through hydrogen-powered anaerobic respiration. KOR expression facilitated CO_2 assimilation and helped retain carbon fluxes within the TCA cycle. Furthermore, the additional expression of ACL preferentially redirected carbon fluxes from the TCA cycle and further channeled them into essential metabolic pathways, including those for protein and nucleotide biosynthesis. These pathways likely play critical roles in sustaining essential reactions under nutrient-limited conditions. The implications of these findings are discussed below.

α-ketoglutarate: ferredoxin oxidoreductase (KOR) supported cellular maintenance of *Escherichia coli* under chemolithotrophic mode

Transcriptome analysis under chemolithotrophic mode was conducted using CO_2 as the sole carbon source after two transgenic *E. coli* strains were constructed. The heterologous genes were well-expressed in two transgenic strains K (*korAB* genes) and KA (*korAB* and *aclBA* genes)

(Table 1b). In enzymatic activity assays, α-ketoglutarate oxidoreductase activity encoded by KOR was significantly higher in the K (49.6 ± 12.2 nmol/min/mg protein, $p = 0.002$) and KA (47.0 ± 16.6 nmol/min/mg protein, $p = 0.008$) strains compared to that of the vector control strain (strain VC, < 0.01), confirming the functionality of the heterologous enzymes in these transgenic strains (Additional file 1: Table S1).

The activities of isocitrate dehydrogenase and isocitrate lyase showed no significant difference between strains VC and K due to their natural presence in *E. coli* [45, 59]. However, four enzymes including α-Ketoglutarate oxidoreductase, isocitrate dehydrogenase, isocitrate lyase, and succinyl-CoA synthetase exhibited higher activity in strain KA compared to strain VC. Notably, succinyl-CoA synthetase activity was significantly higher in the strain KA (9072 ± 522) compared to strain K (5457 ± 674, $p = 0.008$). This increase in activity may be attributed to enhanced acetyl-CoA production driven by ACL expression. Acetyl-CoA, a substrate of malate synthase A (encoded by the *aceB* gene), promotes glyoxylate consumption, which is also a product of isocitrate lyase. As a result, isocitrate lyase activity was marginally higher in strain KA (17.3 ± 3.5, $p = 0.073$) than in strain VC, though not significantly different in strain K (23.2 ± 12.6, $p = 0.280$). The promotion of isocitrate lyase likely increased succinate levels, which serve as the substrate for succinyl-CoA synthetase. This cascade of metabolic changes may explain the significantly enhanced succinyl-CoA synthetase activity observed in strain KA.

To evaluate the role of rTCA machinery under chemolithotrophic conditions, two transgenic *E. coli* strains (K and KA) and a strain with an empty vector (VC) were cultured in an organic-free medium (devoid of organic compounds) under conditions with and without CO_2 supply. The medium was supplemented with hydrogen as the electron donor and nitrate as the electron acceptor for anaerobic respiration. None of the transgenic strains could survive without CO_2 (Fig. 1c, hollow symbols). However, KOR-expressing strains (K and KA) showed an increase in microbial counts under chemolithotrophic conditions with CO_2 supply, in contrast to the VC strain (Fig. 1b, solid symbols). These findings indicate that KOR expression can support cellular maintenance under chemolithotrophic conditions through hydrogen-powered anaerobic respiration.

In previous studies, we introduced four rTCA enzymes into *E. coli* JM109, which successfully assimilated CO_2 with glucose supplementation [40, 60]. Yu et al. introduced five heterologous enzymes (fructose-1,6-bisphosphatase, phosphoribulokinase, fructose-bisphosphate aldolase, ribulose bisphosphate carboxylase, transketolase, and glyceraldehyde-3-phosphate dehydrogenase) from the CBB cycle that enabled CO_2 fixation in the presence of a glucose supply [61]. Gleizer et al. engineered an evolved *E. coli* strain with three additional enzymes including: ribulose-1,5-bisphosphate carboxylase/oxygenase (RuBisCO), phosphoribulokinase through the RuBisCO system, and formate dehydrogenase, enabling autotrophic growth using formate as an energy source [62]. These approaches demonstrated that engineered carbon-fixing *E. coli* strains require multiple heterologous enzymes and supplementation with glucose or formate to accomplish the carbon fixation recycling system and maintain cell viability.

This study is the first to successfully engineer a carbon-fixing *E. coli* capable of sustaining cellular maintenance under chemolithotrophic conditions by introducing a single enzyme (KOR) from rTCA cycle, with CO_2 as the sole carbon source and hydrogen as the energy source. By limiting the heterologous enzyme expression to KOR only, this work achieved carbon fixation, cellular maintenance, and the production of essential metabolites under chemolithotrophic conditions.

Constraint-based flux balance analysis of the reverse tricarboxylic acid cycle machinery in *Escherichia coli*

In-silico modeling was employed to explore potential pathways for CO_2 assimilation in *E. coli* via the rTCA machinery. The predicted pathways for CO_2 assimilation in the *E. coli* strains are illustrated in Additional file 1: Fig. S1. Additional file 1: Tables S2-S4 present the stoichiometric matrix results used in the flux balance analysis aimed at maximizing the biomass reaction rate. The model predicted that CO_2 assimilated by KOR predominantly follows the pathway from glyoxylate to tartronate semialdehyde to glycerate pathway, regulated by glyoxylate carboligase (encoded by the *gcl* gene). To validate the importance of this pathway for transgenic cell survival, this study assessed the cell growth of the *gcl* gene knock-out strains under organic-free conditions in the presence of CO_2. None of the *gcl* gene knock-out strains could survive under these conditions (Additional file 1: Fig. S1b), highlighting the essential role of this pathway. However, further isotopic labeling experiments are needed to quantify the actual metabolic fluxes in transgenic strains.

Expression of α-ketoglutarate: ferredoxin oxidoreductase (KOR) significantly enhanced the incorporation of CO_2 in tricarboxylic acid cycle metabolites

Strains K and KA were cultured under organic-free conditions with $^{13}CO_2$ supplementation. The potential and actual incorporations of $^{13}CO_2$ into TCA cycle metabolites are depicted in Fig. 2. Compared to strain KA, strain K exhibited significantly higher enrichments of $^{13}CO_2$ in citrate ($p = 0.004$), succinate ($p = 0.008$), pyruvate

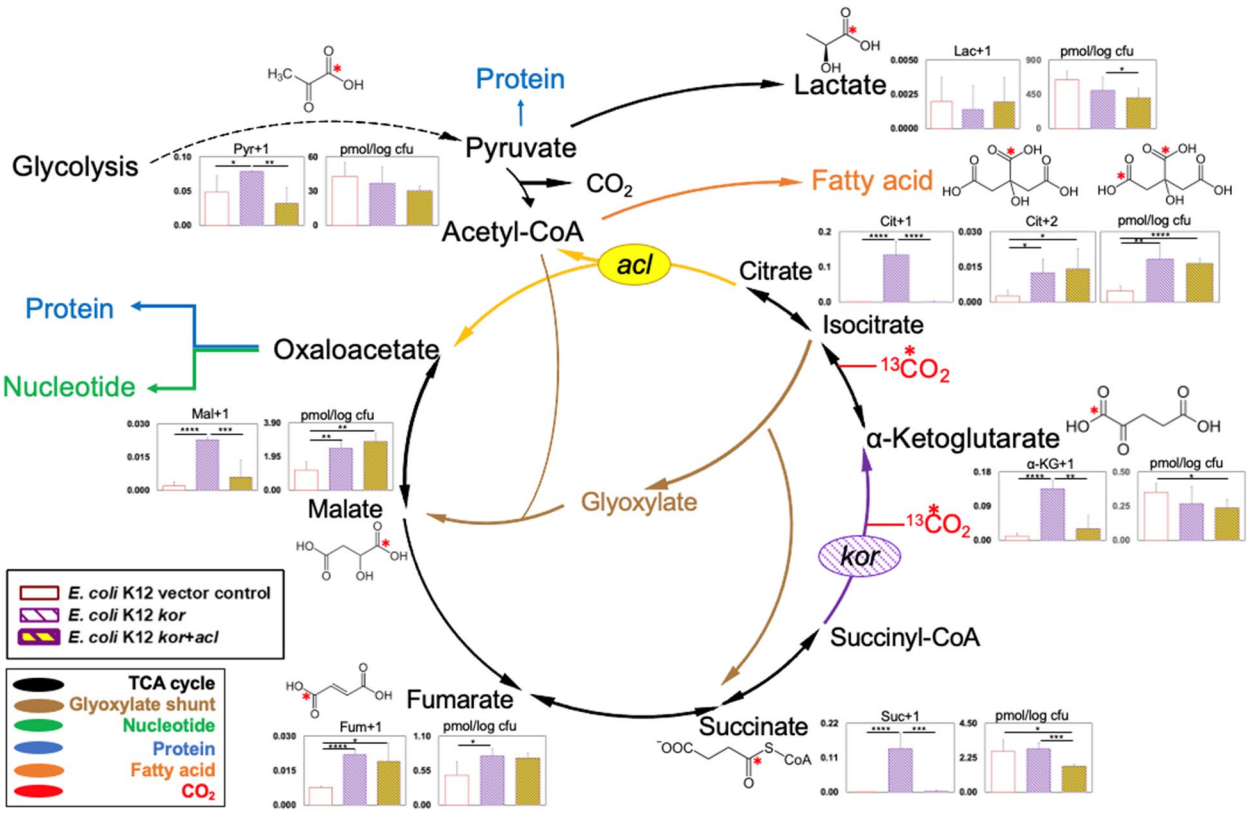

Fig. 2 An overview of the potential metabolic fate of carbon during CO_2 carboxylation in TCA cycle. Isotopic labeling experiments from $^{13}CO_2$ demonstrate the preferential TCA cycle metabolites synthesis and metabolites concentration in transgenic *E. coli* K12. Data are expressed as means standard ± deviation, $n = 3$-4/group. A two-tailed t-test was used for statistical analysis, **** indicates $p < 0.005$ (highly statistically significantly difference); *** indicates $p < 0.01$; ** indicates $p < 0.05$ (statistically significantly difference); * indicates $p < 0.1$ (borderline statistically significantly difference). Strains were supplemented with 10% $^{13}CO_2$ and 90% H_2, re-filled 10% of $^{13}CO_2$ per 12 hr for 48 hr incubation. Isotopic enrichments derived from $^{13}CO_2$ are detected in the M + 1 specie of various organic acid. The labeled $^{13}CO_2$ are marked in red asterisk * marks. Hetero-expressed enzymes: KOR & ACL are marked in purple and yellow, respectively

($p = 0.016$), α-ketoglutarate ($p = 0.005$), and malate ($p = 0.007$). Increased TCA metabolite concentrations were also observed compared to strain VC, especially in fumarate ($p = 0.089$), malate ($p = 0.013$), and citrate ($p = 0.025$).

These results indicate that KOR expression alone effectively enhances the retention of carbon fluxes within the TCA cycle, whereas the addition of ACL might divert the carbon flow away from the TCA (Fig. 2; Table 2). Thus, KOR alone and not KOR + ACL is more effective in maintaining CO_2 fluxes within the TCA cycle compared to KOR + ACL. Further investigation was conducted to explore the role of ACL.

The TCA cycle is a crucial metabolic pathway that integrates carbohydrate, fat, and protein metabolism [63]. Compared to strain VC, the transgenic strain K expressing KOR demonstrated the supporting cellular maintenance under chemolithotrophic conditions. This finding underscores the importance of KOR within the TCA cycle for CO_2 assimilation. The fact that a single enzyme (encoded by two genes) can drive the core reactions in the TCA cycle is noteworthy. α-ketoglutarate, the product of the KOR reaction, is one of the five universal metabolic precursors, as shown through chemical reactions [38], suggesting that the reactions encoded by the *korAB* genes closely resemble metabolic processes. The *in-silico* modeling of strain K proposed an alternative metabolic pathway where glyoxylate is converted to glycerate 2-phosphate. The glyoxylate shunt is an anabolic pathway within the TCA cycle in *E. coli*, which synthesizes components of proteins and the pyrimidines under limited carbon source incubation [64, 65]. This pathway may support cell survival under nutrient-scarce conditions. Metabolic studies further confirmed that KOR expression enhanced the metabolic flux toward glyoxylate, accumulating key metabolites such as citrate, malate, and fumarate. With only one exogenous enzyme for CO_2 fixation, *E. coli* can activate the glyoxylate shunt and replenish critical TCA metabolites. The activation of the glyoxylate shunt by

Table 2 Isotopic labeling experiments from $^{13}CO_2$ demonstrate the preferential TCA cycle metabolites synthesis and metabolites concentration in transgenic *E. Coli* K12

	Pyr[1]	**Pyr + 1**[2]	**Lac**	**Lac + 1**
Strain VC[3]	42.89 ± 12.27	0.048 ± 0.024	637.39 ± 121.82	0.0020 ± 0.0018
Strain K[4]	36.89 ± 14.14	0.079 ± 0.001	499.13 ± 179.39	0.0014 ± 0.0017
P-value[6]	0.584	0.074	0.306	0.696
Strain KA[5]	30.15 ± 4.36	0.032 ± 0.023	404.89 ± 123.97	0.0019 ± 0.0018
P-value[6]	0.165	0.417	0.081	0.981
KA vs. K[7]	0.470	0.016	0.474	0.715
	α-KG	α-KG + 1	Suc	Suc + 1
Strain VC	0.35 ± 0.07	0.010 ± 0.009	2.67 ± 0.75	0.0001 ± 0.0002
Strain K	0.27 ± 0.12	0.135 ± 0.023	2.83 ± 0.41	0.1387 ± 0.0487
P-value	0.346	< 0.001	0.719	0.002
Strain KA	0.24 ± 0.06	0.010 ± 0.009	1.70 ± 0.11	0.0020 ± 0.0034
P-value	0.097	0.604	0.075	0.303
KA vs. K	0.715	0.005	0.006	0.008
	Fum	Fum + 1	Mal	Mal + 1
Strain VC	0.48 ± 0.21	0.008 ± 0.0001	1.16 ± 0.50	0.002 ± 0.002
Strain K	0.78 ± 0.11	0.022 ± 0.002	2.43 ± 0.39	0.023 ± 0.001
P-value	0.089	< 0.001	0.013	< 0.001
Strain KA	0.75 ± 0.08	0.019 ± 0.008	2.82 ± 0.46	0.006 ± 0.008
P-value	0.105	0.056	0.013	0.431
KA vs. K	0.703	0.499	0.281	0.007
	Cit	Cit + 1	Cit + 2	
Strain VC	1.57 ± 0.77	0.0003 ± 0.0005	0.003 ± 0.002	
Strain K	6.11 ± 2.33	0.1338 ± 0.0386	0.012 ± 0.006	
P-value	0.025	0.004	0.052	
Strain KA	5.49 ± 0.70	0.0006 ± 0.0011	0.014 ± 0.008	
P-value	0.001	0.659	0.086	
KA vs. K	0.631	0.004	0.790	

Data are expressed as mean ± SD ($n = 3$–4/group) and compared by Student's t-test

[1] The quantitation (pmol/log cfu) in Pyr (pyruvate), Lac (lactate), α-KG (α-ketoglutarate), Suc (succinate), Fum (fumarate), Mal (malate), Cit (citrate) produced by *E. coli* are shown in grey background

[2] The enrichments in Pyr (pyruvate), α-KG (α-ketoglutarate), Suc (succinate), Fum (fumarate), Mal (malate), Cit (citrate) derived from $^{13}CO_2$ are shown

[3] Strain VC: *E. coli* K12 vector control

[4] Strain K: *E. coli* K12 *korAB* (+) strain

[5] Strain KA: *E. coli* K12 *korAB* (+) & *aclBA* (+) strain

[6] Statistically significantly compared to the strain VC at $p < 0.05$; borderline statistical significance compared to strain VC at $0.05 < p \leqq 0.1$

[7] Statistically significantly compared to the strain K at $p < 0.05$; borderline statistical significance compared to strain K at $0.05 < p \leqq 0.1$

KOR expression may mimic the metabolic pathways of ancient microbes [38].

Additional ATP-dependent citrate lyase (ACL) expression rewired carbon flux of CO2

Although the in-silico model predicted that CO_2 flux rates in the TCA cycle would be higher in the strain expressing both KOR and ACL compared to the strain expressing KOR alone (Additional file 1: Table S4), the experimental results were different. In the experiments using a stable isotope tracer, strain K retained a significantly higher amount of labeled CO_2 in α-ketoglutarate + 1, succinate + 1, malate + 1, and citrate + 1, resulting in increased succinate production compared to strain KA (Fig. 2; Table 2). This discrepancy could be due to differences between the modeling and actual situations. The flux balance analysis and models used [66] did not account for cofactors (nicotinamide adenine dinucleotide (NAD^+), $NADP^+$, ATP, and others), water, or H^+, assuming these were sufficiently supplied and did not limit biomass synthesis. Additionally, the anaplerotic reactions from the TCA cycle were not included in the current model, and the actual

experiments provided complementary insights to the *in-silico* model.

Many biosynthetic reactions utilize the TCA cycle molecules as substrates; however, the model did not incorporate the metabolic pathways for amino acid and protein, fatty acid, or nucleotide biosynthesis. The experiments showed that while the transgenic *E. coli* expressing ACL accumulated fewer CO_2 fluxes within the TCA cycle compared to the KOR-only strain, wild-type *E. coli* did not express ACL, and this cannot cleave citrate into acetyl-CoA and oxaloacetate. The additional expression of ACL in strain K appeared to redirect CO_2 flux toward oxaloacetate and aspartate. Given that aspartate is a proteinogenic amino acid [67] vital for protein synthesis in *E. coli* [68], this study further examined the incorporation of CO_2 into cellular proteins.

"Co-expression of ATP-Dependent Citrate Lyase (ACL) and α-Ketoglutarate: Ferredoxin Oxidoreductase (KOR) exhibited limited effect on fatty acid production

ACL catalyzes the ATP-dependent and coenzyme A (CoA)-dependent conversion of citrate to oxaloacetate and acetyl-CoA, which are key precursors for the biosynthesis [69] of fatty acids, cholesterol, and acetylcholine [70, 71]. The possible role of ACL expression in promoting fatty acid synthesis in the transgenic strains was investigated under anaerobic conditions. However, the experiments showed that the concentrations of fatty acid (Additional file 1: Fig. S2a) and SCFAs (Additional file 1: Fig. S2b) did not differ between strains VC and KA. Additionally, the concentration of butyrate (ng/log cfu) in strain KA (63.37 ± 9.42) was lower than strain VC (79.94 ± 3.02, $p = 0.044$), suggesting that ACL expression did not promote fatty acid synthesis under such a scarce environment.

As for the short-chain fatty acids, strain K exhibited a trend of lower levels of formate, acetate, and propionate compared to strain VC and KA ($p < 0.1$), while butyrate levels were significantly lower ($p < 0.05$). This may indicate that the expression of KOR helps keep CO_2-derived fluxes within the TCA cycle at the expanse of reduced synthesis of SCFAs. A previous study showed that *E. coli* can resorb acetate for converting it to acetyl-CoA via acetyl-CoA synthetase (Acs) and utilized it to energy and biosynthetic components through the TCA cycle and the glyoxylate shunt [72]. This aligns with the observed TCA

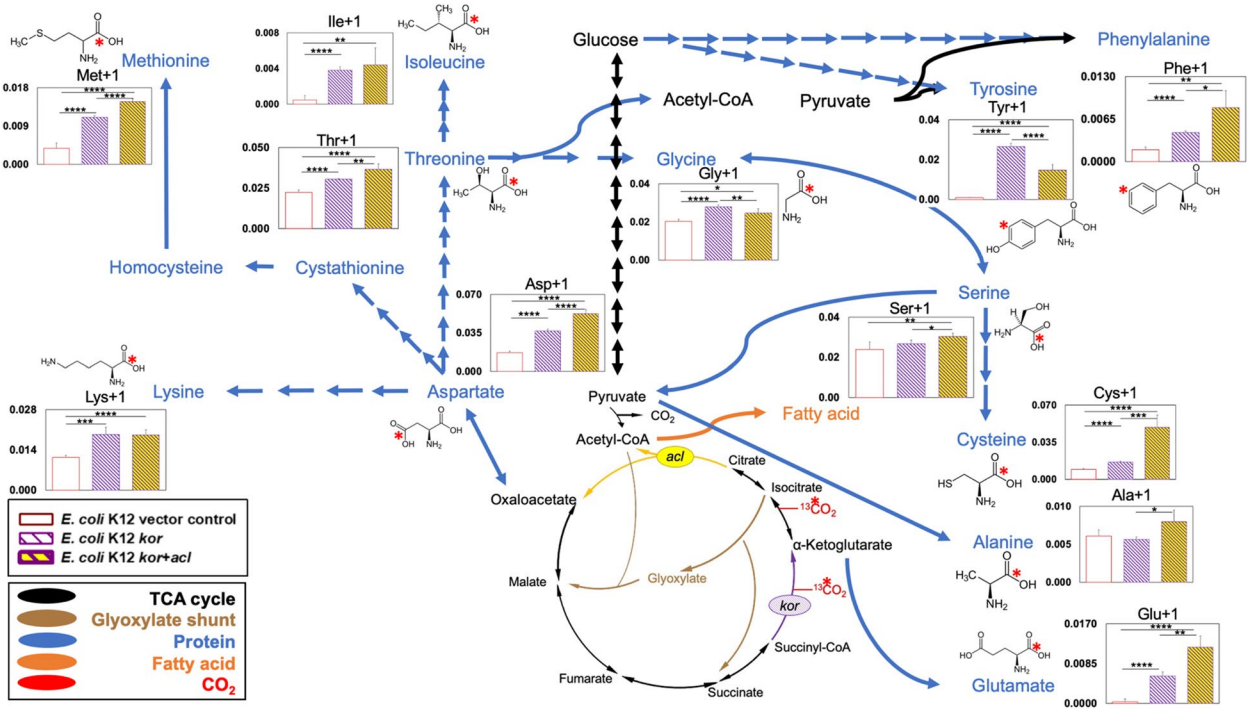

Fig. 3 Incorporation of CO_2 into cellular proteins. The intermediates of the TCA cycle, oxaloacetate and α-ketoglutarate, are metabolized to produce various amino acids, which are subsequently incorporated into cellular proteins. Isotopic labeling experiments using $^{13}CO_2$ demonstrate the preferential synthesis of proteinogenic amino acids in transgenic *E. coli* K12. Data are presented as means ± standard deviation, with $n =$ 3 independent biological samples. A two-tailed t-test was used for statistical analysis, **** indicates $p < 0.005$ (highly statistically significantly difference); *** indicates $p < 0.01$; ** indicates $p < 0.05$ (statistically significantly difference); * indicates $p < 0.1$ (borderline statistically significantly difference). Strains were supplemented with 10% $^{13}CO_2$ and 90% H_2, with 10% of $^{13}CO_2$ replenished every 12 h during the 48 h incubation. Isotopic enrichments derived from $^{13}CO_2$ are detected in the M + 1 specie of various amino acids. The labeled $^{13}CO_2$ are marked in red asterisk * marks. Hetero-expressed enzymes KOR and ACL are indicated in purple and yellow, respectively

cycle metabolite profile in strain K. To sustain KOR activity, strain K appears to use SCFAs as substrates to replenish its carbon source, reflecting a metabolic adaptation to maintain carbon flux under chemolithotrophic conditions.

Co-expression of KOR and ACL restored SCFA levels to values comparable to those of strain VC. Although additional ACL expression in the presence of KOR did modestly enhance SCFA, it did not enhance long chain fatty acid synthesis. Rather, additional ACL expression help re-direct CO_2 metabolic fluxes into nucleotide and protein synthesis.

ATP-dependent citrate lyase (ACL) and α-ketoglutarate: ferredoxin oxidoreductase (KOR) expression assisted $^{13}CO_2$ carbon fixation in protein biosynthesis

ACL cleaves citrate into oxaloacetate and acetyl-CoA, both of which are directly linked to fatty acid turnover in *E. coli* [73]. The similar contents of fatty acid among strains VC, K, and KA suggested that the CO_2 assimilated by KOR was not used for fatty acid with the addition of ACL and that ACL may divert the flow of carbon into other critical metabolic pathways. Consequently, carbon fluxes in cellular protein biosynthesis were experimentally tracked (Fig. 3). As data shown in Fig. 3; Table 3, strain KA exhibited enhanced amino acid enrichments of cellular protein hydrolysates compared to strain K, including threonine + 1, phenylalanine + 1, glycine + 1, isoleucine + 1, methionine + 1, serine + 1, glutamate + 1, cysteine + 1, and alanine + 1. These results suggested that the expression of heterologous KOR with additional ACL, facilitated an increase in CO_2 incorporation in protein biosynthesis.

Expressing ACL in strain K may have been expected to increase fatty acid synthesis due to the greater availability of precursors for fatty acid elongation. However, in this study, the addition of ACL in strain K did not enhance fatty acid production (Additional file 1: Fig. S2). This outcome may be influenced by the presence of inorganic nitrogen ($NaNO_3$) in the culture medium. Nitrogen limitation has been shown to promote fatty acid accumulation in various organisms [74–76]. It is plausible that when nitrogen is abundant, carbon fluxes are more likely to support the synthesis of nitrogen-containing compounds rather than lipid accumulation. These results suggest that carbon flow in strain KA may be redirected toward other metabolic

Table 3 Isotopic labeling experiments from $^{13}CO_2$ demonstrate the preferential proteinic amino acid synthesis in transgenic *E. Coli* K12

	Asp + 1[1]	Glu + 1	Lys + 1	Thr + 1
Strain VC[2]	0.017 ± 0.001	0.000 ± 0.001	0.011 ± 0.001	0.022 ± 0.002
Strain K[3]	0.037 ± 0.002	0.006 ± 0.001	0.019 ± 0.003	0.030 ± 0.000
P-value[5]	< 0.001	0.001	0.006	0.001
Strain KA[4]	0.052 ± 0.004	0.012 ± 0.002	0.019 ± 0.002	0.037 ± 0.003
P-value[5]	< 0.001	0.001	0.002	0.003
KA vs. K[6]	0.003	0.013	0.943	0.034
	Ile + 1	Met + 1	Gly + 1	Ser + 1
Strain VC	0.0005 ± 0.0005	0.004 ± 0.001	0.020 ± 0.001	0.024 ± 0.004
Strain K	0.0038 ± 0.0004	0.011 ± 0.000	0.028 ± 0.001	0.027 ± 0.002
P-value	0.001	0.001	0.001	0.316
Strain KA	0.0044 ± 0.0.0019	0.015 ± 0.001	0.025 ± 0.002	0.030 ± 0.002
P-value	0.026	< 0.001	0.0440	0.048
KA vs. K[6]	0.632	0.001	0.078	0.064
	Cys + 1	Ala + 1	Tyr + 1	Phe + 1
Strain VC	0.009 ± 0.001	0.0061 ± 0.0008	0.010 ± 0.000	0.0018 ± 0.0004
Strain K	0.016 ± 0.001	0.0056 ± 0.0004	0.027 ± 0.002	0.0044 ± 0.0002
P-value	0.001	0.418	< 0.001	0.001
Strain KA	0.049 ± 0.012	0.0080 ± 0.0015	0.015 ± 0.003	0.0082 ± 0.0026
P-value	0.004	0.134	0.001	0.014
KA vs. K[6]	0.008	0.063	0.003	0.067

Data are expressed as mean ± SD ($n = 3$/group) and compared by Student's t-test

[1] The enrichments in Asp (aspartate), Glu (glutamate), Lys (lysine), Thr (threonine), Ile (isoleucine), Met (methionine), Gly (glycine), Ser (serine), Cys (cysteine), Ala (alanine), Tyr (tyrosine), Phe (phenylalanine) derived from $^{13}CO_2$ are shown

[2] Strain VC: *E. coli* K12 vector control

[3] Strain K: *E. coli* K12 *korAB* (+) strain

[4] Strain KA: *E. coli* K12 *korAB* (+) & *aclBA* (+) strain

[5] Statistically significantly compared to the strain VC at $p < 0.05$; borderline statistical significance compared to strain VC at $0.05 < p \leqq 0.1$

[6] Statistically significantly compared to the strain K at $p < 0.05$; borderline statistical significance compared to strain K at $0.05 < p \leqq 0.1$

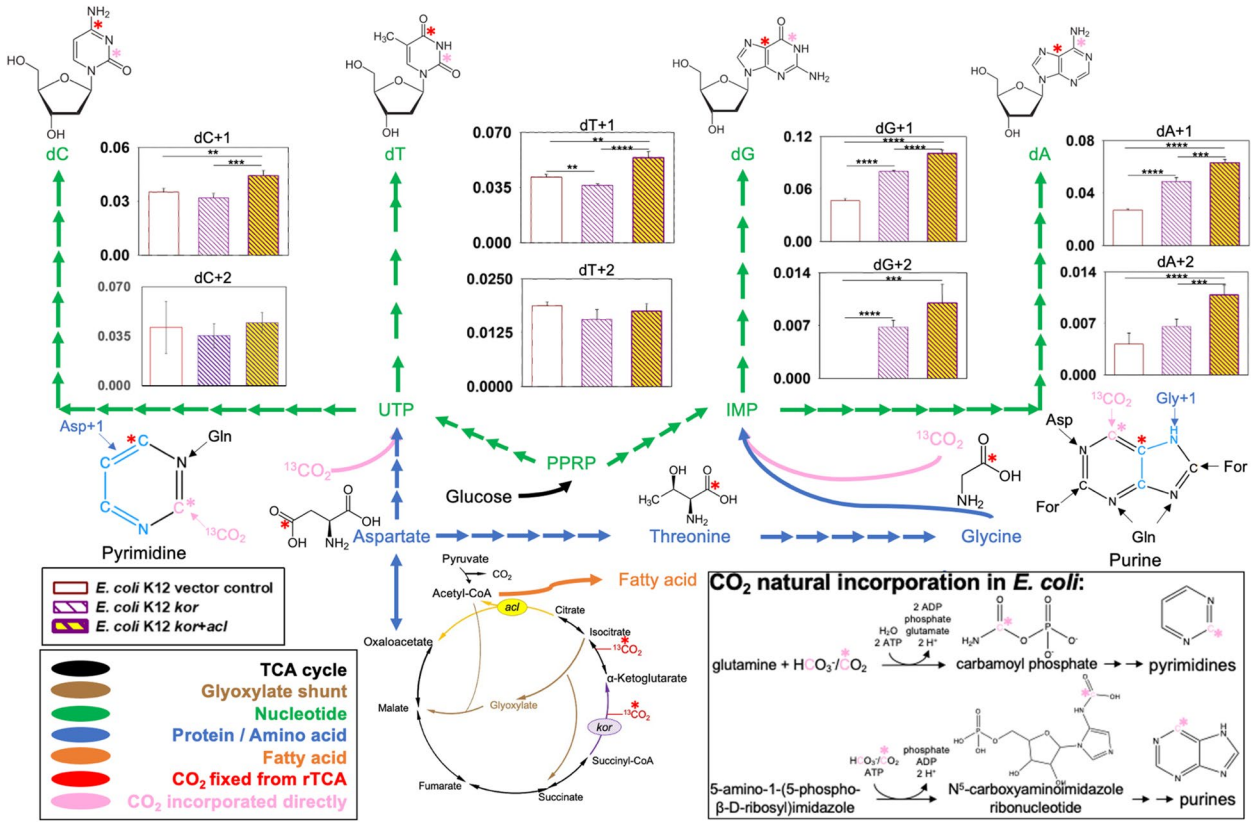

Fig. 4 Incorporation of CO_2 into nucleotides. Effect of hetero-expressed enzymes promote CO_2 incorporation into nucleotides in *E. coli* K12. Data are expressed as means standard ± deviation, $n = 3$ independent biological samples. A two-tailed t-test was used for statistical analysis, **** indicates $p < 0.005$ (highly statistically significantly difference); *** indicates $p < 0.01$; ** indicates $p < 0.05$ (statistically significantly difference); * indicates $p < 0.1$ (borderline statistically significantly difference). Strains were supplemented with 10% $^{13}CO_2$ and 90% H_2, re-filled 10% of $^{13}CO_2$ per 12 hr for 48 hr incubation. Isotopic enrichments derived from $^{13}CO_2$ are detected in the M + 1 or M + 2 specie of various nucleotides. The labeled $^{13}CO_2$ are marked in red asterisk * marks. Hetero-expressed enzymes: KOR & ACL are marked in purple and yellow, respectively. In deoxythymidine and inosine-5′-monophosphate biosynthesis pathway, $^{13}CO_2$ was not incorporated into nucleotide through reverse TCA cycle which are marked in pink asterisk * marks. (Asp: aspartate; Gly: glycine; Gln: glutamine; For: formate; PPRP: phosphoribosyl pyrophosphate; UTP: Uridine triphosphate; IMP: inosine-5′-monophosphate; dC: deoxycytidine; dT: deoxythymidine; dG: deoxyguanosine; dA: deoxyadenosine)

pathways, such as the production of oxaloacetate, a precursor of aspartate. Aspartate is a key compound involved in the synthesis of various metabolites, including amino acids and nucleotides [77, 78]. This redirection aligns with the observed role of ACL in promoting protein biosynthesis over fatty acid production under chemolithotrophic conditions in the presence of $NaNO_3$. Consequently, the effects of KOR and ACL expression on CO_2 incorporation into nucleotides were further investigated.

ATP-dependent citrate lyase (ACL) and α-ketoglutarate: ferredoxin oxidoreductase (KOR) expression assisted $^{13}CO_2$ carbon fixation in nucleotides biosynthesis

Nucleotides, essential for RNA and DNA synthesis and as the primary energy donors for cellular processes [79], were investigated for their biosynthesis in the presence of ACL and KOR. L-aspartate, a substrate of pyrimidine biosynthesis catalyzed by the allosteric enzyme, aspartate transcarbamoylase, is regulated both homotrophically by L-aspartate and heterotrophically by nucleotide effectors such as ATP, CTP (cytidine triphosphate) [80], and UTP (uridine triphosphate) in the presence of CTP [81–83]. It was speculated that ACL also promote nucleotides biosynthesis by increasing the supply of aspartate, a substrate for nucleotides biosynthesis. Although *E. coli* naturally incorporates CO_2 slightly in nucleotide biosynthesis (Fig. 4) [78, 84], it cannot use CO_2 as the sole carbon source for cell growth. When the selected carbon-fixing genes were introduced to the rTCA cycle, the transgenic *E. coli* strains could incorporate more CO_2 into nucleotide structures under nutrient-scarce environments.

A comparison of nucleotide biosynthesis between the two transgenic strains revealed differences. Compared to strains VC and K, the isotopic enrichments in deoxythymidine + 1 (dT + 1) increased by 29% and 48%,

Table 4 Effect of hetero-expressed enzymes promote CO_2 incorporation into nucleotides in *E. Coli* K12

	dC + 1[1]	dC + 2	dT + 1	dT + 2
Strain VC[2]	0.035 ± 0.003	0.041 ± 0.019	0.042 ± 0.002	0.019 ± 0.001
Strain K[3]	0.032 ± 0.003	0.035 ± 0.009	0.036 ± 0.001	0.016 ± 0.003
P-value[5]	0.231	0.647	0.027	0.142
Strain KA[4]	0.044 ± 0.004	0.045 ± 0.007	0.054 ± 0.005	0.018 ± 0.002
P-value[5]	0.024	0.783	0.016	0.386
KA vs. K[6]	0.009	0.226	0.004	0.430
	dG + 1	dG + 2	dA + 1	dA + 2
Strain VC	0.047 ± 0.003	0.000 ± 0.000	0.027 ± 0.001	0.004 ± 0.002
Strain K	0.080 ± 0.002	0.007 ± 0.001	0.049 ± 0.003	0.007 ± 0.001
P-value	< 0.001	< 0.001	< 0.001	0.131
Strain KA	0.101 ± 0.005	0.010 ± 0.003	0.063 ± 0.003	0.011 ± 0.002
P-value	< 0.001	0.005	< 0.001	0.009
KA vs. K[6]	0.002	0.166	0.006	0.021

Data are expressed as mean ± SD ($n = 3$/group) and compared by Student's t-test

[1] The enrichments in dC (deoxycytidine), dT (deoxythymidine), dG (deoxyguanosine), dA (deoxyadenosine) derived from $^{13}CO_2$ are shown

[2] Strain VC: *E. coli* K12 vector control

[3] Strain K: *E. coli* K12 *korAB* (+) strain

[4] Strain KA: *E. coli* K12 *korAB* (+) & *aclBA* (+) strain

[5] Statistically significantly compa-red to the strain VC at $p < 0.05$; borderline statistical significance compared to strain VC at $0.05 < p \leqq 0.1$

[6] Statistically significantly compared to the strain K at $p < 0.05$; borderline statistical significance compared to strain K at $0.05 < p \leqq 0.1$

respectively, in strain KA. Similarly, the isotopic enrichments in deoxycytidine + 1 (dC + 1) increased by 26% and 38%, respectively, in strain KA compared to strains VC and K. Additionally, in the purine biosynthesis pathway, the isotopic enrichments in deoxyadenosine + 1 (dA + 1) increased by 134% and 29%, respectively, in strain KA compared to strains VC and K, while enrichment in dA + 2 was increased by 401% in strain KA compared to strain VC. The enrichments of deoxyguanosine + 1 (dG + 1) increased by 115% and 26% in strain KA compared to strains VC and K, respectively, with dG + 2 being significantly enriched in strain KA compared to that in strain VC (Fig. 4; Table 4). These results suggested that the co-expressions of KOR, and KOR with ACL promoted the incorporation of CO_2 for the biosynthesis of pyrimidines and purine in *E. coli*, with the highest CO_2 incorporation was detected in strain KA.

In *E. coli* and other organisms, CO_2, formate, and glycine are involved in synthesizing the purine ring [85] (Fig. 4). The model indicated an advantage of CO_2 incorporation into purines upon KOR expression. Furthermore, the additional expression of ACL significantly impacted purine synthesis from CO_2. These findings align with the increased enrichment of glycine in cellular proteins and cytoplasmic amino acids. Glycine is a crucial source for purine formation [84], suggesting that ACL and KOR facilitate CO_2 incorporation into purines by improving glycine availability. For pyrimidines, CO_2, aspartate, glutamate, and acetate serve as carbon sources [84] (Fig. 4). Compared to purines, the effects of KOR and ACL on pyrimidines biosynthesis were relatively moderate. These findings are consistent with the similar enrichment of aspartate in cellular protein and cytoplasmic amino acids. Notably, KA exhibited higher enrichments of deoxy-cytosine + 1 and deoxy-thymidine + 1 compared to K and VC, which may partially result from increased CO_2 incorporations into glutamate.

In this study, carbon-fixing *E. coli* transgenic strains capable of assimilating CO_2 via rTCA machinery were successfully constructed. The results demonstrate that expressing either KOR alone or KOR in combination with ACL is sufficient to support cellular maintenance and CO_2 assimilation in *E. coli* under chemolithotrophic conditions. The engineered metabolic pathways in these transgenic strains represent the minimal and essential requirements for sustaining cellular life, closely reflecting the core metabolic functions necessary for survival.

However, achieving indefinite growth of *E. coli* with CO_2 as the sole carbon source remains a significant challenge. According to a previous study [2], α-ketoglutarate: ferredoxin oxidoreductase (KOR) catalyzes the carboxylation of succinyl-CoA to α-ketoglutarate and coenzyme A, utilizing CO_2 and two moles of reduced ferredoxin as substrates. We hypothesize that the primary limitation lies in the insufficient availability of reduced ferredoxin to sustain KOR activity under nutrient-scarce conditions.

(See figure on next page.)

Fig. 5 An overview of the potential metabolic fate of $^{13}CO_2$ during the TCA cycle, cellular protein biosynthesis, nucleotide biosynthesis, and the impact on fatty acid production in transgenic *E. coli* K12 strains expressed (**a**) KOR or (**b**) KOR with ACL compared to vector control strain, respectively. A two-tailed t-test was used for statistical analysis, **** indicates $p < 0.005$ (highly statistically significantly difference);*** indicates $p < 0.01$; ** indicates $p < 0.05$ (statistically significantly difference); * indicates $p < 0.1$ (borderline statistically significantly difference). Two heterologous enzymes, KOR and ACL, play distinct roles in this carbon fixing system. KOR primarily fixes CO_2 through the rTCA cycle, maintaining carbon flow within the TCA cycle. ACL further redirects and shifts the carbon flux of CO_2 out of TCA cycle towards cellular protein and nucleotide biosynthesis. Metabolites from carbohydrate and TCA cycle are denoted in black, amino acids in blue, fatty acids in orange, and labeled $^{13}CO_2$ in red. Hetero-expressed enzymes, KOR and ACL, are represented in purple and yellow, respectively. (SAFA: saturated fatty acids; MUFA: mono-unsaturated fatty acids; TFA: total fatty acid; PPRP: phosphoribosyl pyrophosphate; dC: deoxycytidine; dT: deoxythymidine; dG: deoxyguanosine; dA: deoxyadenosine)

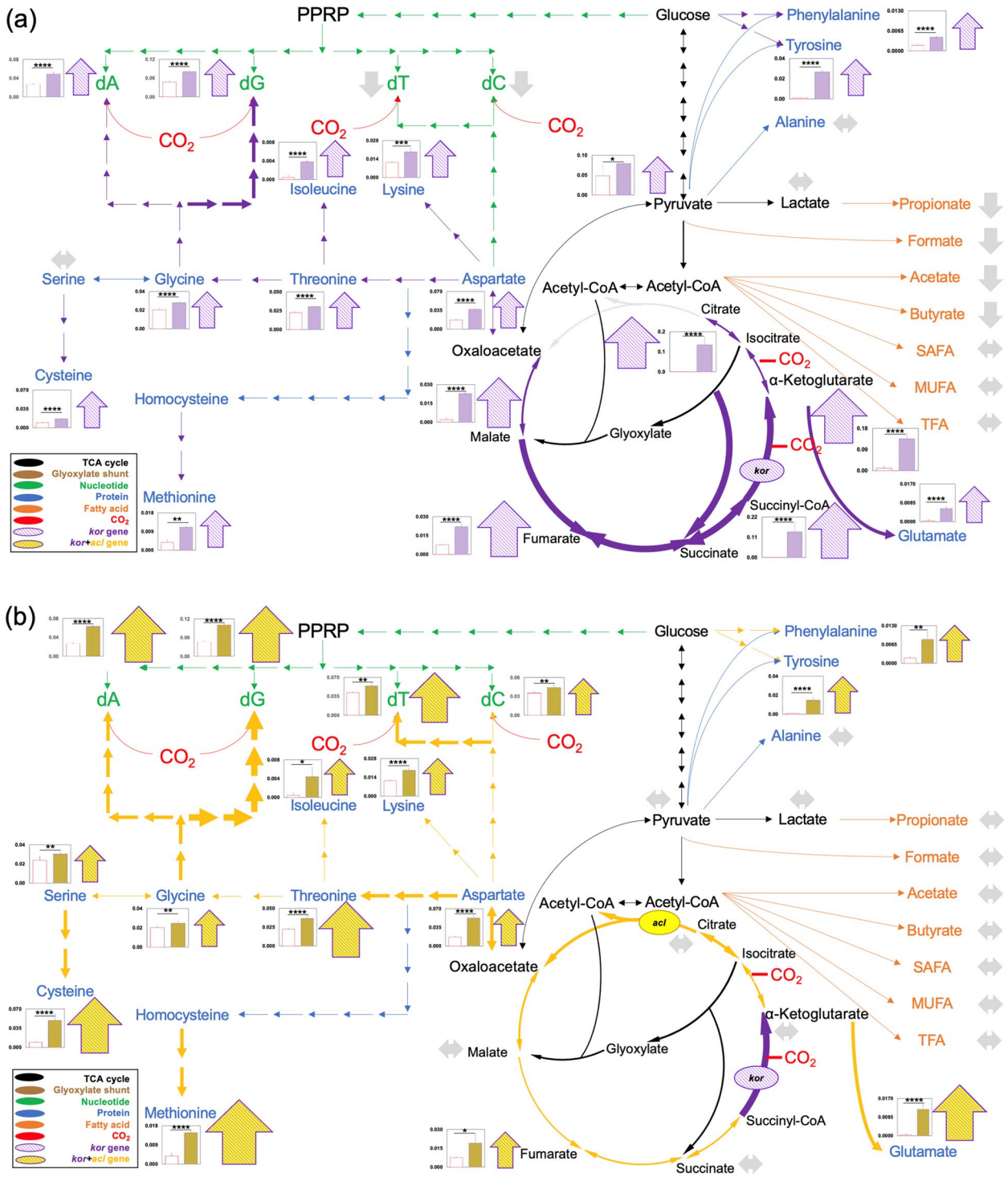

Fig. 5 (See legend on previous page.)

To address this bottleneck and move closer to fully autotrophic growth, future research should focus on increasing the availability of reduced ferredoxin. Potential strategies include engineering pathways to enhance ferredoxin reduction or exploring methods for external supplementation of reducing power. These efforts could pave the way for transgenic strains capable of achieving complete autotrophic growth in fully organic-free environments.

Conclusion

This study is the first to successfully engineer a carbon-fixing *E. coli* strain capable of cellular maintenance under chemolithotrophic conditions with hydrogen-powered anaerobic respiration by adding only one enzyme. The expression of KOR facilitates CO_2 assimilation and carbon fluxes retention within the TCA cycle (Fig. 5a). Moreover, the additional expression of ACL further directs carbon fluxes into essential cellular processes such as protein and nucleotide biosynthesis (Fig. 5b). The metabolic pathways assembled in the transgenic *E. coli* strains are deemed essential and represent a minimal configuration for cell living, closely reflecting core metabolism functions.

Abbreviations

rTCA	reverse tricarboxylic acid
KOR	α-ketoglutarate: ferredoxin oxidoreductase
ACL	ATP-dependent citrate lyase
FR	fumarate reductase
SDH	succinate dehydrogenase
LUCA	last universal common ancestor
CBB	Calvin-Benson-Bassham
RNA	ribonucleic acid
TCA	tricarboxylic acid
MTBSTFA	N-tert-Butyldimethylsily-N-methyltrifluoroacetamide
PFBBr	pentafluorobenzyl bromide
DMSO	Dimethyl sulfoxide
OGAB	Ordered Gene Assembly in the Bacillus subtilis
DNA	deoxyribonucleic acid
O.D.	optical density
cfu	colony-forming units
NADP	Nicotinamide adenine dinucleotide phosphate
ATP	adenosine triphosphate
GC-MS	gas chromatography-mass spectrometry
SCFAs	short-chain fatty acids
MS	Mass spectrometry
dA	deoxyadenylate
dG	deoxyguanylate
dT	deoxythymidine
dC	deoxycytidine
VC	vector control
CoA	coenzyme A
CTP	cytidine triphosphate
UTP	uridine triphosphate
RuBisCO	ribulose-1,5-bisphosphate carboxylase/oxygenase
NAD	nicotinamide adenine dinucleotide

Supplementary Information

The online version contains supplementary material available at https://doi.org/10.1186/s13036-025-00489-w.

Supplementary Material 1.

Acknowledgements

Not applicable.

Authors' contributions

J.H.P. performed the experiments, analyzed the data, and prepared the manuscript. Y.N.Y., S.C.L., and Y.C.C. performed the experiments and analyzed the data. E.P.I.C., and C.C.H. analyzed the data and prepared the manuscript. Y.T.Y., A.I.T., and T.T.S. analyzed data. D.Y.W., C.H.Y., and C.H.H. performed experiments. All authors have read and agreed to the published version of the manuscript.

Funding

This work was supported by National Science and Technology Council (NSTC) 110-2320-B-005-008-MY3 (E.-P.I.C.), 110-2320-B-005-003-MY3 (E.-P.I.C.), 110-2321-B-005-008 (E.-P.I.C., C.-C.H., Y.-T.Y.), 107-2621-M-005-008-MY3 (E.-P.I.C., C.-C.H., Y.-T.Y.), 107-2621-M-005-007-MY3 (C.-C.H.), 107-2321-B-005-009 (E.-P.I.C., C.-C.H.), 107-2320-B-005-003-MY3 (E.-P.I.C., C.-C.H.), 106-2221-E-005-007-MY3 (C.-C.H), 104-2621-M-005-003-MY3 (C.-C.H.). It is also funded in part by the "Innovation and Development Center of Sustainable Agriculture (IDCSA)" and the "Advanced Plant and Food Crop Biotechnology Center (APFCBC) from The Featured Areas Research Center Program within the framework of the Higher Education Sprout Project by the Ministry of Education (MOE) (E.-P.I.C., C.-C.H.) in Taiwan.

Data availability

No datasets were generated or analysed during the current study.

Declarations

Ethics approval and consent to participate

Not applicable.

Consent for publication

Not applicable.

Competing interests

The authors declare no competing interests.

Author details

[1]Doctoral Program in Microbial Genomics, National Chung Hsing University and Academia Sinica, Taichung City and Taipei City 402 and 115, Taiwan. [2]Department of Life Sciences, National Chung Hsing University, Taichung City 402, Taiwan. [3]Department of Electrical Engineering, National Tsing Hua University, Hsinchu City 30013, Taiwan. [4]Advanced Plant and Food Crop Biotechnology Center, National Chung Hsing University, Taichung City 402, Taiwan. [5]Innovation and Development Center of Sustainable Agriculture, National Chung Hsing University, Taichung City 402, Taiwan. [6]Department of Food Science and Biotechnology, National Chung Hsing University, Taichung City 402, Taiwan.

Received: 13 November 2024 Accepted: 10 February 2025
Published online: 26 February 2025

References

1. van Soest HL, den Elzen MGJ, van Vuuren DP. Net-zero emission targets for major emitting countries consistent with the Paris agreement. Nat Commun. 2021;12(1):2140. https://doi.org/10.1038/s41467-021-22294-x.
2. Hügler M, Wirsen CO, Fuchs G, Taylor CD, Sievert SM. Evidence for autotrophic CO_2 fixation via the reductive tricarboxylic acid cycle by members of the Epsilon subdivision of proteobacteria. J Bacteriol. 2005;187(9):3020–7. https://doi.org/10.1128/JB.187.9.3020-3027.2005.
3. Liang B, Zhao Y, Yang J. Recent advances in developing artificial autotrophic microorganism for reinforcing CO_2 fixation. Front Microbiol. 2020;11:592631. https://doi.org/10.3389/fmicb.2020.592631.
4. Kelly DP. Autotrophy: concepts of lithotrophic bacteria and their organic metabolism. Annu Rev Microbiol. 1971;25:177–210. https://doi.org/10.1146/annurev.mi.25.100171.001141.
5. Rabus R, Hansen TA, Widdel F. Dissimilatory sulfate- and sulfur-reducing prokaryotes. In: Rosenberg E, DeLong EF, Lory S, Stackebrandt E, Thompson F, editors. The prokaryotes: prokaryotic physiology and biochemistry. Berlin, Heidelberg: Springer Berlin Heidelberg; 2013. p. 309–404.
6. Robertson LA, Kuenen JG. The colorless sulfur bacteria. In: Dworkin M, Falkow S, Rosenberg E, Schleifer KH, Stackebrandt E, editors. The prokaryotes: volume 2: ecophysiology and biochemistry. New York: Springer New York; 2006. p. 985–1011.
7. Dar R, Bandh SA, Shafi S, Shameem N. Chapter 2 - bacterial diversity of the rock-water interface in freshwater ecosystem. In: Bandh SA, Shafi S, Shameem N, editors. Freshwater microbiology. Cambridge: Academic Press; 2019. p. 73–104. https://doi.org/10.1016/B978-0-12-817495-1.00002-5.

8. Adamczyk PA, Reed JL. *Escherichia coli* as a model organism for systems metabolic engineering. Curr Opini Systems Biology. 2017;6:80–8. https://doi.org/10.1016/j.coisb.2017.11.001.
9. Weiss MC, Preiner M, Xavier JC, Zimorski V, Martin WF. The last universal common ancestor between ancient earth chemistry and the onset of genetics. PLoS Genet. 2018;14(8): e1007518. https://doi.org/10.1371/journal.pgen.1007518.
10. Chong PK, Burja AM, Radianingtyas H, Fazeli A, Wright PC. Proteome and transcriptional analysis of ethanol-grown *Sulfolobus solfataricus* P2 reveals ADH2, a potential alcohol dehydrogenase. J Proteome Res. 2007;6(10):3985–94. https://doi.org/10.1021/pr070232y.
11. Auernik KS, Kelly RM. Physiological versatility of the extremely thermoacidophilic archaeon *Metallosphaera sedula* supported by transcriptomic analysis of heterotrophic, autotrophic, and mixotrophic growth. Appl Environ Microbiol. 2010;76(3):931–5. https://doi.org/10.1128/AEM.01336-09.
12. Strauss G, Eisenreich W, Bacher A, Fuchs G. ^{13}C-NMR study of autotrophic CO_2 fixation pathways in the sulfur-reducing Archaebacterium *Thermoproteus neutrophilus* and in the phototrophic Eubacterium *Chloroflexus aurantiacus*. Eur J Biochem. 1992;205(2):853–66. https://doi.org/10.1111/j.1432-1033.1992.tb16850.x.
13. Sirevåg R, Buchanan BB, Berry JA, Troughton JH. Mechanisms of CO_2 fixation in bacterial photosynthesis studied by the carbon isotope fractionation technique. Arch Microbiol. 1977;112(1):35–8. https://doi.org/10.1007/BF00446651.
14. Ragsdale SW. Pyruvate ferredoxin oxidoreductase and its radical intermediate. Chem Rev. 2003;103(6):2333–46. https://doi.org/10.1021/cr020423e.
15. Thauer RK, Kaster AK, Seedorf H, Buckel W, Hedderich R. Methanogenic archaea: ecologically relevant differences in energy conservation. Nat Rev Microbiol. 2008;6(8):579–91. https://doi.org/10.1038/nrmicro1931.
16. Alber BE, Kung JW, Fuchs G. 3-Hydroxypropionyl-coenzyme A synthetase from *Metallosphaera sedula*, an enzyme involved in autotrophic CO_2 fixation. J Bacteriol. 2008;190(4):1383–9. https://doi.org/10.1128/JB.01593-07.
17. Hattori S, Galushko AS, Kamagata Y, Schink B. Operation of the CO dehydrogenase/acetyl coenzyme A pathway in both acetate oxidation and acetate formation by the syntrophically acetate-oxidizing bacterium *Thermacetogenium phaeum*. J Bacteriol. 2005;187(10):3471–6. https://doi.org/10.1128/JB.187.10.3471-3476.2005.
18. Ettema TJ, Makarova KS, Jellema GL, Gierman HJ, Koonin EV, Huynen MA, et al. Identification and functional verification of archaeal-type phosphoenolpyruvate carboxylase, a missing link in archaeal central carbohydrate metabolism. J Bacteriol. 2004;186(22):7754–62. https://doi.org/10.1128/JB.186.22.7754-7762.2004.
19. Martins BM, Dobbek H, Cinkaya I, Buckel W, Messerschmidt A. Crystal structure of 4-hydroxybutyryl-CoA dehydratase: radical catalysis involving a [4Fe-4S] cluster and flavin. Proc Natl Acad Sci U S A. 2004;101(44):15645–9. https://doi.org/10.1073/pnas.0403952101.
20. Evans MC, Buchanan BB, Arnon DI. A new ferredoxin-dependent carbon reduction cycle in a photosynthetic bacterium. Proc Natl Acad Sci U S A. 1966;55(4):928–34. https://doi.org/10.1073/pnas.55.4.928.
21. Siebers B, Schönheit P. Unusual pathways and enzymes of central carbohydrate metabolism in Archaea. Curr Opin Microbiol. 2005;8(6):695–705. https://doi.org/10.1016/j.mib.2005.10.014.
22. Huber C, Wächtershäuser G. Activated acetic acid by carbon fixation on (Fe,Ni)S under primordial conditions. Science. 1997;276(5310):245–7. https://doi.org/10.1126/science.276.5310.245.
23. Ivanovsky RN, Fal YI, Berg IA, Ugolkova NV, Krasilnikova EN, Keppen OI, et al. Evidence for the presence of the reductive pentose phosphate cycle in a filamentous anoxygenic photosynthetic bacterium, *Oscillochloris trichoides* strain DG-6. Microbiol (Reading). 1999;145(Pt 7):1743–8. https://doi.org/10.1099/13500872-145-7-1743.
24. Auernik KS, Maezato Y, Blum PH, Kelly RM. The genome sequence of the metal-mobilizing, extremely thermoacidophilic archaeon *Metallosphaera sedula* provides insights into bioleaching-associated metabolism. Appl Environ Microbiol. 2008;74(3):682–92. https://doi.org/10.1128/AEM.02019-07.
25. Teufel R, Kung JW, Kockelkorn D, Alber BE, Fuchs G. 3-hydroxypropionyl-coenzyme A dehydratase and acryloyl-coenzyme A reductase, enzymes of the autotrophic 3-hydroxypropionate/4-hydroxybutyrate cycle in the *Sulfolobales*. J Bacteriol. 2009;191(14):4572–81. https://doi.org/10.1128/JB.00068–09.
26. Bassham JA, Benson AA, Calvin M. The path of carbon in photosynthesis. J Biol Chem. 1950;185(2):781–7.
27. Berg IA, Kockelkorn D, Ramos-Vera WH, Say RF, Zarzycki J, Hugler M, et al. Autotrophic carbon fixation in archaea. Nat Rev Microbiol. 2010;8(6):447–60. https://doi.org/10.1038/nrmicro2365.
28. Hügler M, Sievert SM. Beyond the Calvin cycle: autotrophic carbon fixation in the ocean. Ann Rev Mar Sci. 2011;3:261–89. https://doi.org/10.1146/annurev-marine-120709-142712.
29. Fuchs G. Alternative pathways of carbon dioxide fixation: insights into the early evolution of life? Annu Rev Microbiol. 2011;65:631–58. https://doi.org/10.1146/annurev-micro-090110-102801.
30. Braakman R, Smith E. The emergence and early evolution of biological carbon-fixation. PLoS Comput Biol. 2012;8(4):e1002455. https://doi.org/10.1371/journal.pcbi.1002455.
31. Raven JA. The role of autotrophs in global CO_2 cycling. In: Lidstrom ME, Tabita FR, editors. Microbial growth on C_1 compounds: Proceedings of the 8th International Symposium on Microbial Growth on C_1 Compounds, held in San Diego, USA, 27 August – 1 September 1995. Dordrecht: Springer Netherlands; 1996. p. 351–8.
32. Shively JM, English RS, Baker SH, Cannon GC. Carbon cycling: the prokaryotic contribution. Curr Opin Microbiol. 2001;4(3):301–6. https://doi.org/10.1016/s1369-5274(00)00207-1.
33. Häder DP. Photosynthesis in plants and Algae. Anticancer Res. 2022;42(10):5035–41. https://doi.org/10.21873/anticanres.16012.
34. Boyle NR, Morgan JA. Computation of metabolic fluxes and efficiencies for biological carbon dioxide fixation. Metab Eng. 2011;13(2):150–8. https://doi.org/10.1016/j.ymben.2011.01.005.
35. Kitadai N, Maruyama S. Origins of building blocks of life: a review. Geosci Front. 2018;9(4):1117–53. https://doi.org/10.1016/j.gsf.2017.07.007.
36. Muchowska KB, Varma SJ, Chevallot-Beroux E, Lethuillier-Karl L, Li G, Moran J. Metals promote sequences of the reverse Krebs cycle. Nat Ecol Evol. 2017;1(11):1716–21. https://doi.org/10.1038/s41559-017-0311-7.
37. Braakman R, Smith E. The compositional and evolutionary logic of metabolism. Phys Biol. 2013;10(1): 011001. https://doi.org/10.1088/1478-3975/10/1/011001.
38. Muchowska KB, Varma SJ, Moran J. Synthesis and breakdown of universal metabolic precursors promoted by iron. Nature. 2019;569(7754):104–7. https://doi.org/10.1038/s41586-019-1151-1.
39. Mayer RJ, Moran J. Quantifying reductive amination in nonenzymatic amino acid synthesis. Angew Chem Int Ed Engl. 2022;61(48): e202212237. https://doi.org/10.1002/anie.202212237.
40. Lo S-C, Chiang E-PI, Yang Y-T, Li S-Y, Peng J-H, Tsai S-Y, et al. Growth enhancement facilitated by gaseous CO_2 through Heterologous expression of reductive tricarboxylic acid cycle genes in *Escherichia coli*. Fermentation. 2021;7(2):98. https://doi.org/10.3390/fermentation7020098.
41. Nishizaki T, Tsuge K, Itaya M, Doi N, Yanagawa H. Metabolic engineering of carotenoid biosynthesis in *Escherichia coli* by ordered gene assembly in *Bacillus subtilis*. Appl Environ Microbiol. 2007;73(4):1355–61. https://doi.org/10.1128/AEM.02268-06.
42. Ohashi Y, Hirayama A, Ishikawa T, Nakamura S, Shimizu K, Ueno Y, et al. Depiction of metabolome changes in histidine-starved *Escherichia coli* by CE-TOFMS. Mol Biosyst. 2008;4(2):135–47. https://doi.org/10.1039/b714176a.
43. Cheng YC, Huang WH, Lo SC, Huang E, Chiang EI, Huang CC, et al. Conversion of *Escherichia coli* into Mixotrophic CO_2 assimilation with malate and hydrogen based on recombinant expression of 2-oxoglutarate:Ferredoxin oxidoreductase using adaptive laboratory evolution. Microorganisms. 2023;11(2). https://doi.org/10.3390/microorganisms11020253.
44. Lebedeva NV, Malinina NV, Ivanovskii RN. A comparative study of the isocitrate dehydrogenases of *Chlorobium limicola* forma *Chlorobium thiosulfatophilum* and *Rhodopseudomonas palustris*. Mikrobiologiia. 2002;71(6):762–7. https://doi.org/10.1023/A:1021471621183.
45. Prasad Maharjan R, Yu PL, Seeto S, Ferenci T. The role of isocitrate lyase and the glyoxylate cycle in *Escherichia coli* growing under glucose limitation. Res Microbiol. 2005;156(2):178–83. https://doi.org/10.1016/j.resmic.2004.09.004.
46. Cha S, Parks RE Jr. Succinic Thiokinase. I. Purification of the enzyme from pig heart. J Biol Chem. 1964;239:1961–7. https://doi.org/10.1016/S0021-9258(18)91291-3.
47. Zhang J, Ahn WS, Gameiro PA, Keibler MA, Zhang Z, Stephanopoulos G. ^{13}C isotope-assisted methods for quantifying glutamine metabolism in cancer cells. Methods Enzymol. 2014;542:369–89. https://doi.org/10.1016/B978-0-12-416618-9.00019-4.
48. Morita M, Gravel SP, Chenard V, Sikstrom K, Zheng L, Alain T, et al. mTORC1 controls mitochondrial activity and biogenesis through 4E-BP-dependent

translational regulation. Cell Metab. 2013;18(5):698–711. https://doi.org/10.1016/j.cmet.2013.10.001.
49. Lamarre SG, MacMillan L, Morrow GP, Randell E, Pongnopparat T, Brosnan ME, et al. An isotope-dilution, GC-MS assay for formate and its application to human and animal metabolism. Amino Acids. 2014;46(8):1885–91. https://doi.org/10.1007/s00726-014-1738-7.
50. Bligh EG, Dyer WJ. A rapid method of total lipid extraction and purification. Can J Biochem Physiol. 1959;37(8):911–7. https://doi.org/10.1139/o59-099.
51. Metcalfe LD, Schmitz AA, Pelka JR. Rapid preparation of fatty acid esters from lipids for gas chromatographic analysis. Anal Chem. 1966;38(3):514–5. https://doi.org/10.1021/ac60235a044.
52. Ostermann AI, Muller M, Willenberg I, Schebb NH. Determining the fatty acid composition in plasma and tissues as fatty acid methyl esters using gas chromatography - a comparison of different derivatization and extraction procedures. Prostaglandins Leukot Essent Fat Acids. 2014;91(6):235–41. https://doi.org/10.1016/j.plefa.2014.10.002.
53. Ackman RG, Sipos JC. Application of specific response factors in the gas chromatographic analysis of methyl esters of fatty acids with flame ionization detectors. J Am Oil Chem Soc. 1964;41(5):377–8. https://doi.org/10.1007/BF02654818.
54. Craske JD, Bannon CD. Letter to the editor. J Am Oil Chemists' Soc. 1988;65(7):1190–1. https://doi.org/10.1007/BF02660581.
55. Tumanov S, Bulusu V, Kamphorst JJ. Analysis of fatty acid metabolism using stable isotope Tracers and Mass Spectrometry. Methods Enzymol. 2015;561:197–217. https://doi.org/10.1016/bs.mie.2015.05.017.
56. Tan YL, Sou NL, Tang FY, Ko HA, Yeh WT, Peng JH, et al. Tracing metabolic fate of mitochondrial Glycine cleavage system derived Formate in Vitro and in vivo. Int J Mol Sci. 2020;21(22): 8808. https://doi.org/10.3390/ijms21228808.
57. Hsu FY, Liou JY, Tang FY, Sou NL, Peng JH, Chiang EI. Ketogenic diet consumption inhibited mitochondrial one-carbon metabolism. Int J Mol Sci. 2022;23(7). https://doi.org/10.3390/ijms23073650.
58. Wu MT, Ye WT, Wang YC, Chen PM, Liu JY, Tai CK, et al. MTHFR knockdown assists cell defense against folate depletion induced chromosome segregation and uracil misincorporation in DNA. Int J Mol Sci. 2021;22(17). https://doi.org/10.3390/ijms22179392.
59. Lee ME, Dyer DH, Klein OD, Bolduc JM, Stoddard BL, Koshland DE Jr. Mutational analysis of the catalytic residues lysine 230 and tyrosine 160 in the $NADP^+$-dependent isocitrate dehydrogenase from *Escherichia coli*. Biochemistry. 1995;34(1):378–84. https://doi.org/10.1021/bi00001a046.
60. Chen CH, Tseng IT, Lo SC, Yu ZR, Pang JJ, Chen YH, et al. Manipulating ATP supply improves in situ CO_2 recycling by reductive TCA cycle in engineered *Escherichia coli*. 3 Biotech. 2020;10(3):125. https://doi.org/10.1007/s13205-020-2116-7.
61. Yu J, Shin WR, Kim JH, Lee SY, Cho BK, Kim YH, et al. Increase CO_2 recycling of *Escherichia coli* containing CBB genes by enhancing solubility of multiple expressed proteins from an operon through temperature reduction. Microbiol Spectr. 2023;11(6):e0256023. https://doi.org/10.1128/spectrum.02560-23.
62. Gleizer S, Ben-Nissan R, Bar-On YM, Antonovsky N, Noor E, Zohar Y, et al. Conversion of *Escherichia coli* to generate all biomass carbon from CO_2. Cell. 2019;179(6):1255–63 e12. https://doi.org/10.1016/j.cell.2019.11.009.
63. Sweetlove LJ, Beard KF, Nunes-Nesi A, Fernie AR, Ratcliffe RG. Not just a circle: flux modes in the plant TCA cycle. Trends Plant Sci. 2010;15(8):462–70. https://doi.org/10.1016/j.tplants.2010.05.006.
64. Kornberg HL. The role and control of the glyoxylate cycle in *Escherichia coli*. Biochem J. 1966;99(1):1–11. https://doi.org/10.1042/bj0990001.
65. Maloy SR, Nunn WD. Genetic regulation of the glyoxylate shunt in *Escherichia coli* K-12. J Bacteriol. 1982;149(1):173. https://doi.org/10.1128/jb.149.1.173-180.1982.
66. Cheng HTY, Lo SC, Huang CC, Ho TY, Yang YT. Detailed profiling of carbon fixation of *in silico* synthetic autotrophy with reductive tricarboxylic acid cycle and Calvin-Benson-Bassham cycle in *Esherichia coli* using hydrogen as an energy source. Synth Syst Biotechnol. 2019;4(3):165–72. https://doi.org/10.1016/j.synbio.2019.08.003.
67. Piao X, Wang L, Lin B, Chen H, Liu W, Tao Y. Metabolic engineering of *Escherichia coli* for production of L-aspartate and its derivative beta-alanine with high stoichiometric yield. Metab Eng. 2019;54:244–54. https://doi.org/10.1016/j.ymben.2019.04.012.
68. Micaletto M, Fleurier S, Dion S, Denamur E, Matic I. The protein carboxymethyltransferase-dependent aspartate salvage pathway plays a crucial role in the intricate metabolic network of *Escherichia coli*. Sci Adv. 2024;10(6):eadj0767. https://doi.org/10.1126/sciadv.adj0767.
69. Chypre M, Zaidi N, Smans K. ATP-citrate lyase: a mini-review. Biochem Biophys Res Commun. 2012;422(1):1–4. https://doi.org/10.1016/j.bbrc.2012.04.144.
70. Sun J, Pan CQ, Chew TW, Liang F, Burmeister M, Low BC. BNIP-H recruits the cholinergic machinery to neurite terminals to promote acetylcholine signaling and neuritogenesis. Dev Cell. 2015;34(5):555–68. https://doi.org/10.1016/j.devcel.2015.08.006.
71. Verschueren KHG, Blanchet C, Felix J, Dansercoer A, De Vos D, Bloch Y, et al. Structure of ATP citrate lyase and the origin of citrate synthase in the Krebs cycle. Nature. 2019;568(7753):571–5. https://doi.org/10.1038/s41586-019-1095-5.
72. Kumari S, Beatty CM, Browning DF, Busby SJ, Simel EJ, Hovel-Miner G, et al. Regulation of acetyl coenzyme a synthetase in *Escherichia coli*. J Bacteriol. 2000;182(15):4173–9. https://doi.org/10.1128/JB.182.15.4173–4179.2000.
73. Zhao L, Zhao X, Wu J, Lou X, Yang H. Comparison of metabolic response between the planktonic and air-dried *Escherichia coli* to electrolysed water combined with ultrasound by ^{1}H NMR spectroscopy. Food Res Int. 2019;125:108607. https://doi.org/10.1016/j.foodres.2019.108607.
74. Lv G, Xu Y, Tu Y, Cheng X, Zeng B, Huang J, et al. Effects of nitrogen and phosphorus limitation on fatty acid contents in *Aspergillus oryzae*. Front Microbiol. 2021;12:739569. https://doi.org/10.3389/fmicb.2021.739569.
75. Yang ZK, Niu YF, Ma YH, Xue J, Zhang MH, Yang WD, et al. Molecular and cellular mechanisms of neutral lipid accumulation in diatom following nitrogen deprivation. Biotechnol Biofuels. 2013;6(1): 67. https://doi.org/10.1186/1754-6834-6-67.
76. Chen X, He Y, Liu L, Zhu X, Sen B, Wang G. Nitrogen starvation enhances the production of saturated and unsaturated fatty acids in *Aurantiochytrium* sp. PKU#SW8 by regulating key biosynthetic genes. Mar Drugs. 2022;20(10):621. https://doi.org/10.3390/md20100621.
77. Liu F, Qimuge, Hao J, Yan H, Bach T, Fan L, et al. AspC-mediated aspartate metabolism coordinates the *Escherichia coli* cell cycle. PLoS One. 2014;9(3):e92229. https://doi.org/10.1371/journal.pone.0092229.
78. Roberts RB, Cowie DB, Britten R, Bolton E, Abelson PH. The role of the tricarboxylic acid cycle in amino acid synthesis in *Escherichia coli*. Proc Natl Acad Sci U S A. 1953;39(10):1013–9. https://doi.org/10.1073/pnas.39.10.1013.
79. Kilstrup M, Hammer K, Ruhdal Jensen P, Martinussen J. Nucleotide metabolism and its control in lactic acid bacteria. FEMS Microbiol Rev. 2005;29(3):555–90. https://doi.org/10.1016/j.femsre.2005.04.006.
80. Gerhart JC, Pardee AB. The enzymology of control by feedback inhibition. J Biol Chem. 1962;237:891–6. https://doi.org/10.1016/S0021-9258(18)60389-8.
81. Wild JR, Loughrey-Chen SJ, Corder TS. In the presence of CTP, UTP becomes an allosteric inhibitor of aspartate transcarbamoylase. Proc Natl Acad Sci U S A. 1989;86(1):46–50. https://doi.org/10.1073/pnas.86.1.46.
82. Sakash JB, Kantrowitz ER. The N-terminus of the regulatory chain of *Escherichia coli* aspartate transcarbamoylase is important for both nucleotide binding and heterotropic effects. Biochemistry. 1998;37(1):281–8. https://doi.org/10.1021/bi972102g.
83. Schubert C, Zedler S, Strecker A, Unden G. L-Aspartate as a high-quality nitrogen source in *Escherichia coli*: regulation of L-aspartase by the nitrogen regulatory system and interaction of L-aspartase with GlnB. Mol Microbiol. 2021;115(4):526–38. https://doi.org/10.1111/mmi.14620.
84. Bolton E. Biosynthesis of nucleic acid in *Escherichia coli*. Proc Natl Acad Sci U S A. 1954;40(8):764–72. https://doi.org/10.1073/pnas.40.8.764.
85. Weed LL, Wilson DW. The incorporation of C^{14}-orotic acid into nucleic acid pyrimidines in vitro. J Biol Chem. 1951;189(1):435–42. https://doi.org/10.1016/S0021-9258(18)56135-4.

Publisher's Note

Springer Nature remains neutral with regard to jurisdictional claims in published maps and institutional affiliations.